



ELSEVIER

Available online at www.sciencedirect.com



Journal of Molecular Structure xxx (2006) xxx–xxx

Journal of
MOLECULAR
STRUCTURE

www.elsevier.com/locate/molstruc

Silicon nanocrystals by thermal annealing of Si-rich silicon oxide prepared by the LPCVD method

M. Ivanda^{a,*}, H. Gebavi^a, D. Ristić^a, K. Furić^a, S. Musić^a, M. Ristić^a, S. Žonja^b,
P. Biljanović^b, O. Gamulin^c, M. Balarin^c, M. Montagna^d, M. Ferarri^e, G.C. Righini^f

^a Ruđer Bošković Institute, P.O. Box 180, 10002 Zagreb, Croatia

^b Faculty for Electrotechnic and Computing, University of Zagreb, Unska 3, 10000 Zagreb, Croatia

^c Medical School, Department of Physics and Biophysics, University of Zagreb, Salata 3b, 10000, Zagreb, Croatia

^d Dipartimento di Fisica, Università di Trento and INFN, I-38050 Povo, Trento, Italy

^e Istituto di Fotonica e Nanotecnologie, CSMFO group, Via Sommarive 14, Trento, I-38050 Trento, Italy

^f Department of Optoelectronics and Photonics, Nello Carrara Institute of Applied Physics, IFAC – CNR, Via Panciatichi 64, I-50127 Firenze, Italy

Received 8 September 2006; received in revised form 28 September 2006; accepted 28 September 2006

14 Abstract

15 The Si-rich silicon oxide (SiO_x) thin films are prepared on silicon crystalline substrates by low pressure chemical vapor deposition
16 (LPCVD) method. The oxygen concentration x are controlled by the ratio of the partial pressures of N_2O and SiH_4 gases in the reaction
17 chamber. In order to induce the phase separation on SiO_2 and Si nanostructures the samples are annealed at the temperatures 900–
18 1100 °C. The structural and optical properties of the samples are investigated by Raman and infrared spectroscopy and scanning electron
19 microscopy.

20 © 2006 Published by Elsevier B.V.

21 *Keywords:* Si-rich silicon oxide; LPCVD; Raman scattering; Low frequency particle modes

23 1. Introduction

24 The growth of thin films by low pressure chemical vapor
25 deposition (LPCVD) is one of the most important tech-
26 niques for deposition of thin films in modern technology.
27 The reasons of a broad application of the LPCVD method
28 are in possibility of deposition of different elements and
29 compounds at relatively low temperatures in amorphous
30 and crystalline phase with high degree of uniformity and
31 purity. A simple handling, high reliability of operations,
32 fast deposition, homogeneity of deposited layers and high
33 reproducibility are the basic characteristics the LPCVD
34 method.

35 Apart from vitreous silica as the archetypal oxide net-
36 work former and the basis of traditional silicate glasses

other amorphous oxides of silicon such as silicon monoxide 37
and silicon sesquioxide (Si_2O_3) also exists. These amor- 38
phous silicon suboxides have been known for decades 39
and are used in a variety of technical applications. The pos- 40
sibility of phase separation of silicon suboxides into silicon 41
and SiO_2 was first proposed by Brady [1]. On the basis of a 42
theoretical approach this concept was discussed in more 43
detail by Temkin [2] who proposed a random-mixture 44
(RM) model. The RM model assumes small domains in 45
which either silicon is bonded only to silicon or to oxygen. 46
This corresponds to a two-phase mixture of Si and SiO_2 47
domains with thin boundary layer of ≈ 10 Å between [2]. 48
Dupree et al. [3] performed magic-angle spinning (MAS) 49
NMR investigations on silicon monoxide and estimated 50
phase separated regions of Si and SiO_2 near to 20 Å. 51

In this paper we show the results of the LPCVD deposi- 52
tion of non stoichiometric oxide SiO_x thin films with SiH_4 53
and N_2O precursors. The chemical reaction we used is oxi- 54

* Corresponding author.

E-mail address: ivanda@irb.hr (M. Ivanda).

55 dation of silane with N_2O : $SiH_4 + \gamma N_2O \rightarrow p-$
 56 $SiO_x + (1 - p)SiH_4 + 2pH_2 + (\gamma - px)N_2O + px N_2$. The
 57 silicon nanocrystals were formed by phase separation of
 58 SiO_x ($x < 2$) structure induced by thermal annealing:
 59 $SiO_x \rightarrow (1 - x/2) Si + x/2 SiO_2$, where N_2O/SiH_4 ratio con-
 60 trols the Si amount in the layer.

61 2. Experimental

62 The LPCVD method is most successfully applied in
 63 deposition of polysilicon thin films from SiH_4 in the tem-
 64 perature range 580–660 °C and SiO_2 layers from SiH_2Cl_2
 65 at 900 °C. The scheme of the conventional hot-wall hori-
 66 zontal LPCVD reactor is shown in Fig. 1. The base of
 67 device is a quartz tube placed in a spiral heater. The tube
 68 is evacuated on the pressure of 0.1 Pa and heated on to
 69 the wanted temperature to 1000 °C. The temperature sta-
 70 bility is ± 1 °C. The deposition starts with entering of
 71 the working gas in the tube. The working (dynamical) pressure
 72 is 10–200 Pa.

73 In this experiment the non-stoichiometric oxide SiO_x
 74 ($x < 2$) were deposited on 0.65 μm thick thermal oxide on
 75 a (111) oriented silicon substrate with a diameter of
 76 50 mm set at 7 mm from the 1st (dummy) wafer. The depo-
 77 sitions were carried out by thermal decomposition of 2%
 78 (S1) and 26% silane (S2 and S3) diluted in argon. The depo-
 79 sition temperatures was 748 °C. The flow rate ratios of
 80 nitrous oxide and silane $\Phi(N_2O)/\Phi(SiH_4)$ are presented in
 81 Table 1. The SiO_x films were further thermally annealed
 82 at 900, 1000 and 1100 °C in air. Upon annealing the
 83 decomposition of SiO_x into SiO_2 and elemental Si takes
 84 place. After the decomposition, the excess Si atoms form
 85 Si clusters embedded in a SiO_2 matrix. The size of Si clus-
 86 ters is expected to become larger for the higher annealing
 87 temperatures. The deposited layers were characterized by
 88 Raman spectroscopy using Dilor Z-24 Raman triple mono-

Table 1

Deposition parameters of SiO_x thin films

Sample	$\Phi(SiH_4)/sccm$	$\Phi(N_2O)/\Phi(SiH_4)$
S1	6.2	4.04
S2	37.7	1.14
S3	80.5	1.03

chromator spectrometer, IR absorption spectroscopy and 89
 scanning electron microscopy (SEM). 90

91 3. Results and discussion

92 The main difference between CVD depositions at low 92
 pressure and atmospheric pressure is in ratio of the mass 93
 transport velocity and the velocity of reaction on the sur- 94
 face. At atmospheric pressure these quantities are of the 95
 same order of magnitude. While the velocity of the mass 96
 transport depends mainly on the reactant concentration, 97
 diffusion, and thickness of the border layer, the velocity 98
 of the surface reaction depends mainly on the concentra- 99
 tion of reactants and temperature. As diffusion of gas is 100
 reciprocal to pressure, it will decrease 1000 times if the 101
 pressure reduces from atmospheric value to 100 Pa. Now 102
 the carrier gas is not more necessary, the substrates could 103
 approach more closely, and deposited films shows better 104
 uniformity and homogeneity. The working gas, that regu- 105
 larly consist of the gas for dilution and of the reactive 106
 gas, after entering spreads inside the tube and flows above 107
 the hot substrates (thin wafers of silicon, quartz or some 108
 other material) placed in the quartz holders. The wafers 109
 in the tube reactor are radiantly heated by resistive hearing 110
 coils surrounding the tube. The critical factors that influ- 111
 ence on thickness uniformity and film content are positions 112
 of the substrates, temperature profile in the zone of deposi- 113
 tion, reactor geometry, deposition time, working pressure, 114
 as well as the quantity and content of all gases or vapors 115
 that enter in the reactor. 116

117 Fig. 2a shows the FTIR spectrum of the sample S1. The 117
 band above 1000 cm^{-1} is assigned to the asymmetric 118
 stretching of the Si–O–Si bridge. This peak position can 119
 be used for reasonable stoichiometry estimation in case 120
 of a homogeneous SiO_x alloy [4]. The observed peak posi- 121
 tion at 1072 cm^{-1} , which differs from the position of ther- 122
 mally grown oxide at $\sim 1080\text{ cm}^{-1}$, gives the composition 123
 $x = 1.9$. The SEM image in Fig. 2b shows that the layer 124
 is porous and in homogeneous. These results show that 125
 the structure of deposited layer is more close to the silica 126
 structure than to SiO structure. 127

128 In order to decrease the composition x we have 128
 decreased the flow rate ratio to: $\Phi(N_2O)/\Phi(SiH_4) = 1.14$ 129
 (sample S2). Fig. 3 shows the Raman spectra of as depos- 130
 ited and annealed samples. The Raman spectra shows the 131
 characteristic bands of SiO_x structure that consists of the 132
 broad peaks at 160 and 460 cm^{-1} which corresponds to 133
 the TO and TA phonon-like bands. Upon thermal anneal- 134
 ing the decomposition of SiO_x into SiO_2 and elemental Si 135

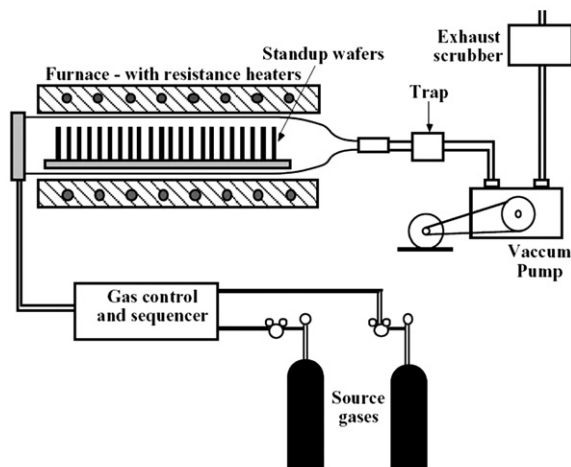


Fig. 1. Schematic description of the LPCVD device.

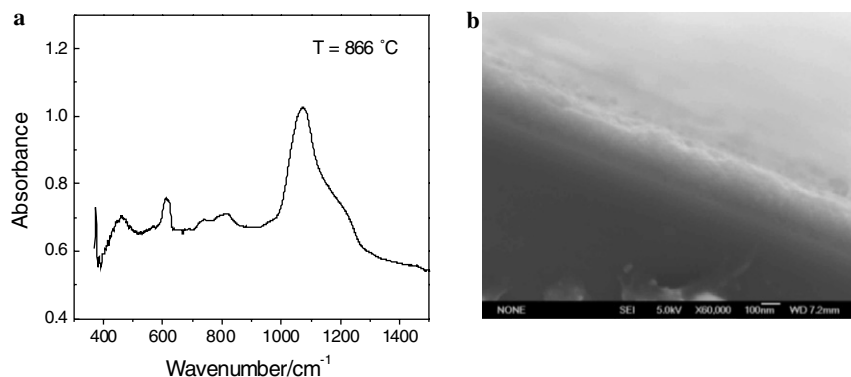


Fig. 2. FTIR spectrum (a) and SEM image (b) of the sample S1.

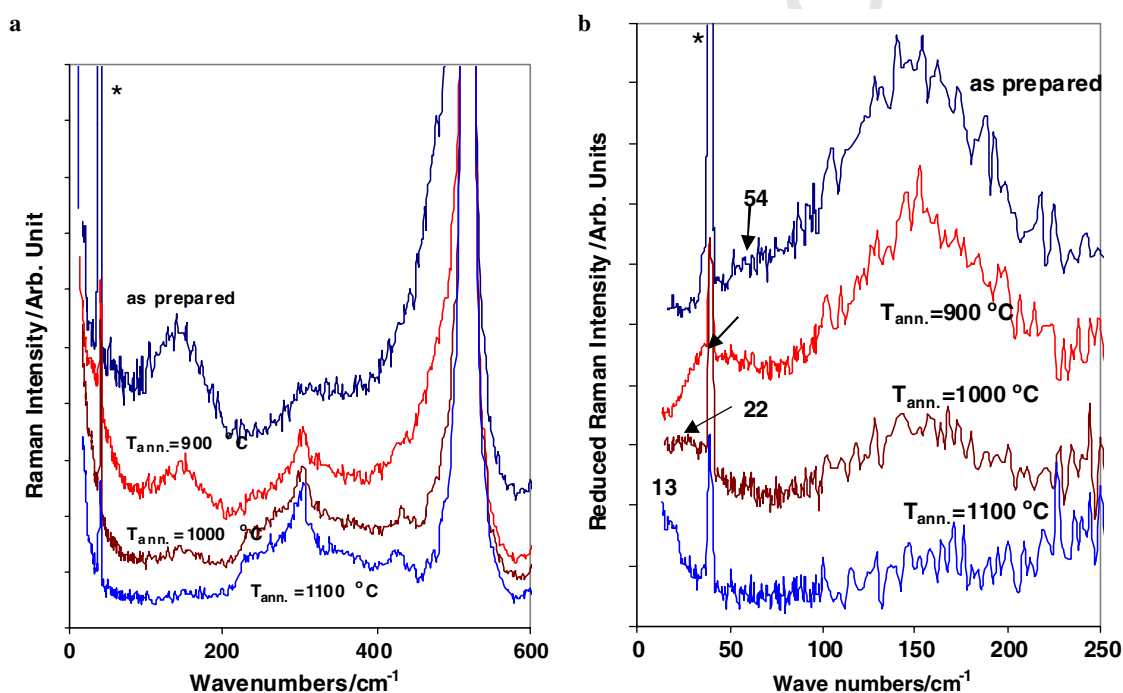


Fig. 3. Raman spectra of SiO_x structure in the range of TA and TO phonon-like bands of the sample deposited at 748°C with the gas flow rate ratio $\Phi(\text{N}_2\text{O})/\Phi(\text{SiH}_4) = 1.14$ (a); the low frequency reduced Raman spectra of the same samples (b) the arrow indicate the symmetric vibrational mode of silicon nanoparticles. The asterisk indicates the plasma line at 39 cm^{-1} .

136 takes place. After decomposition, the excess Si atoms form
 137 Si clusters embedded in a SiO_2 matrix. The size of Si clus-
 138 ters is expected to become larger for higher annealing tem-
 139 peratures. The Raman scattering on nanosized silicon
 140 particle manifests in broadening and red shift of the
 141 TO(γ) phonon band at 521 cm^{-1} and blue shift of the
 142 low frequency spherical mode with decrease of particle size.
 143 The model of phonon confinement of optical modes [5] and
 144 the calculation of spherical acoustical modes are applied in
 145 order to deduce the mean size and distribution width of sil-
 146 icon nanocrystals [6].

147 Low frequency modes indicated by an arrow in Fig. 3b
 148 corresponds to the spherical acoustical modes of silicon
 149 nanocrystals. Vibrations of elastic spheres have been stud-
 150 ied for a long time by Lamb [7]. The frequency (in wave-
 151 numbers) of the symmetric spherical mode is given by [8]:

$$v_0 = \frac{S_0 v_L}{cD}, \quad (1)$$

where v_0 is the frequency of the surface symmetric modes, 155
 D is the diameter of the spherical particle and c is the veloc- 156
 ity of light. The constant $S_0 = 0.76$ [6]. The mean value of 157
 the longitudinal sound velocities calculated across three 158
 crystalline directions is $v_L = 8790\text{ m/s}$. These parameters 159
 when inserted in Eq. (1) give the mean size of silicon nano- 160
 particles from the know frequency of the symmetric spheri- 161
 cal mode, i.e. $D = 2.29 \times 10^{-7}/v_0$. Experimentally, by 162
 comparison of the low frequency Raman results with the 163
 particles size distributions obtained by TEM, the size of sil- 164
 icon particles deduced by Eq. (1) are by the factor of 0.5 165
 smaller [6]. The reason for such factor is still unclear and 166
 could be connected with the resonance phenomena of inci- 167

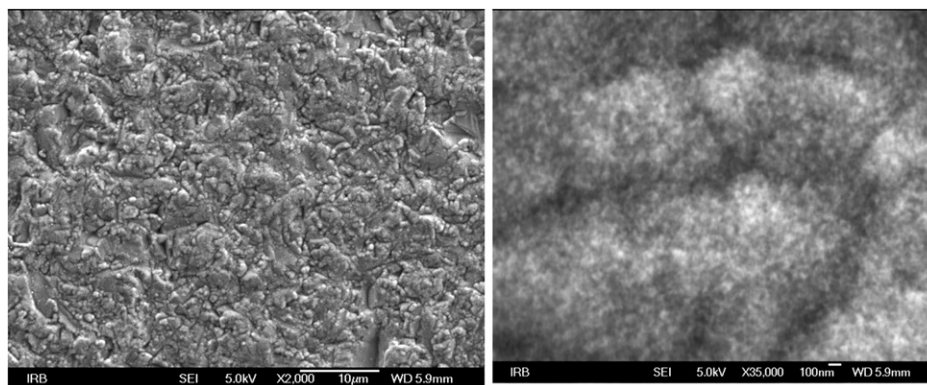


Fig. 4. SEM images of the SiO_x film prepared at 748 °C by silane reaction with N_2O at flow rate: $\Phi(\text{SiH}_4) = 80.5$ sccm, and gas flow rate ratio: $\Phi(\text{N}_2\text{O})/\Phi(\text{SiH}_4) = 1.03$.

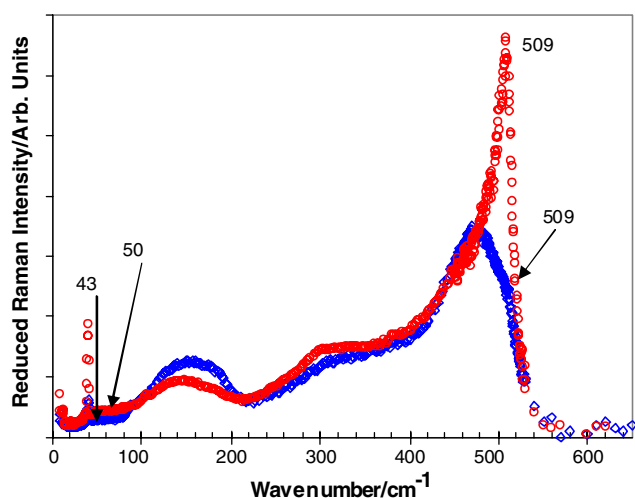


Fig. 5. Raman spectra reduced for the Bose–Einstein factor of SiO_x prepared with silane flow rate $\Phi(\text{SiH}_4) = 80.5$ sccm, and gas flow rate ratio: $\Phi(\text{N}_2\text{O})/\Phi(\text{SiH}_4) = 1.03$ (circles) and of the same sample annealed at 900 °C for 1 h in air (diamonds). The asterisk indicates the plasma line at 39 cm^{-1} .

dent laser energy with the exciton transition in silicon [6]. Taking this into the consideration, the silicon nanocrystals with mean sizes of 3.2, 5.2 and 8.8 nm are formed in the films annealed at 900, 1000 and 1100 °C, respectively. Some broad bands with maximum at 54 cm^{-1} also exist for the as deposited samples. This could be also ascribed to spherical vibrations that correspond to the broad distribution of silicon nanoparticles. The mean particles size of 2.2 nm estimated from the peak maximum agree with the value obtained by NMR measurements of Dupree et al. [3].

With further decrease of the flow rate ratio to $\Phi(\text{N}_2\text{O})/\Phi(\text{SiH}_4) = 1.03$ (sample S3), the black porous structure with porous surface morphology shown in Fig. 4 is obtained. The sample is then further annealed at 900 °C for 1 h in air. The low frequency Raman spectra of the as deposited and annealed sample shows the broad peaks of spherical modes peak with maximums at 43 and 50 cm^{-1} which corresponds to the mean particle size of 2.7 and 2.3 nm, respectively. The existence of such small crystallites

are also confirmed by the Raman scattering on the confined TO(Γ) phonon mode that appear as a shoulder and sharp peak at 509 cm^{-1} of the as prepared and annealed sample. By applying the phonon confinement model, the mean particle size is possible to obtain by the relation [5]: $D = 0.337/(521/\nu - 1)$, where ν is observed frequency of TO(Γ) phonon mode. The particles of mean size of 1.4 nm were found by this formula which is similar to those found from the LFR modes Fig. 5.

As a conclusion here we have shown that by using LPCVD technique a number of different silicon SiO_x nanostructures important for microelectronic and photonic application is possible to prepare with rather simple approach. The content of oxygen atoms is possible to control by of nitrous oxide and silane partial pressure gas ratio and the particle size by the temperature of annealing process. The different size of silicon nanocrystals in silica matrix are obtained by subsequent annealing of SiO_x structure. The Raman scattering techniques showed to be simple and reliable technique in determination of size of prepared silicon nanoparticles.

Acknowledgement

This work was supported by the Ministry of Science and Technology of the Republic of Croatia.

References

- [1] G.W. Brady, J. Phys. Chem. 63 (1959) 1119.
- [2] R.J. Temkin, J. Non-Cryst. Solids 17 (1975) 215.
- [3] R. Dupree, D. Holland, D.S. Williams, Philos. Mag. Lett. B 50 (3) (1984) L13.
- [4] Y. Kanzawa, S. Hayashi, K. Yamamoto, J. Phys.: Condens. Matter 8 (1996) 4823–4835.
- [5] Ch. Ossadnik, S.Veprek, I. Gregora, Thin Solid Films, 1999.
- [6] M. Ivanda, A. Hohl, M. Montagna, G. Mariotto, M. Ferrari, Z. Crnjak Orel, A. Turković, K. Furić, J. Raman Spectrosc. 37 (2006) 161–165.
- [7] H. Lamb, Proc. Math. Soc. London 13 (1882) 187.
- [8] M. Ivanda, K. Babocsi, C. Dem, M. Schmitt, M. Montagna, W. Kiefer, Phys. Rev. B 67 (2003) 235329.